GEOLOGICAL SURVEY OF
DENMARK AND GREENLAND
Report 1996/16

Annealing cosimulating of Dan Field chalk matrix permeability with Simulated porosity

Report to Project: EFP95 1313/95-0005

By Ole Valdemar Vejbæk

GEUS

GEOLOGICAL SURVEY OF
DENMARK AND GREENLAND
Report 1996/16

Annealing cosimulating of Dan Field chalk matrix permeability with Simulated porosity

Report to Project: EFP95 1313/95-0005

By Ole Valdemar Vejbæk

GEUS
Geological Survey of
Denmark and Greenland

Annealing cosimulation of Dan Field chalk matrix permeability with simulated porosity.

Ole Valdemar Vejbæk

March 13, 1996

Report to Project: EFP95 1313/95-0005

Geostatistical reservoir characterization using inverted seismic data; application to a chalk reservoir, Dan Field, Denmark

Geological survey of Denmark and Greenland, Ministry of the Environment (GEUS)

Contents

1 Abstract

Permeabilities in a part of the Maastrichtian reservoir unit on the southern flank of the Dan Field are simulated by the use an annealing cosimulation (ACS) technique. Coredata from the 15 available wells within the volume is scarce, so simulation of the permeability distribution is conditioned to a combination of only few hard data, an a priori obtained spatial porosity description, variogram structures, a histogram and a constructed bivariate conditioning distribution. Scarcity of core analysis (hard) data is a problem that is overcome by the construction of a conditioning bivariate dataset of porosity and permeability.

2 Introduction

The purpose of this report is to present the application of an annealing cosimulation (ACS) technique to derive a spatial permeability description of matrix properties in a chalk volume, where porosities are already described. The ACS technique is described in more detail by Deutsch and Cockerham (1994), and further information can be obtained from Deutsch and Journel (1992).

This report constitutes a continuation of the work carried out by Vejbæk (1995; Vejbæk and Rasmussen, in press) where the porosity in a volume of chalk was simulated by the use of a gaussian collocated cosimulation algoritm. These porosities are available a priori and are used as soft data in this report. The cosimulation of porosities applied seismic impedances as secondary (soft) data to constrain the solution. The area of interest is thus identical to that of the earlier study (Fig. 1), and the simulation volume is also identical in location and size (Fig. 2). The simulated volume comprises only the Maastrichtian and is rotated approximately 45° from north because of the orientation of the 3D seismic dataset that was used for support in deriving the three-dimensional porosity description (Vejbæk 1995). The thickness of the simulated volume is 107m, which encompasses Maastrichtian units 1 to 6 as defined by Kristensen et al. (1995). The well data base used is the same as in the earlier report and comprises fifteen wells which all are in public domain. They are: M8x, Md1, Me3, Me6, Mfa6, Mfa8, Mfb1, Mfb4a, Mfb7, Mfb8, Mfb9, Mfb10, Mfb11, Mfb12, and Mfb14b. Although production from the reservoir relies heavily of fractures (mainly artificially induced; Jørgensen 1992), this study only deals with matrix properties.

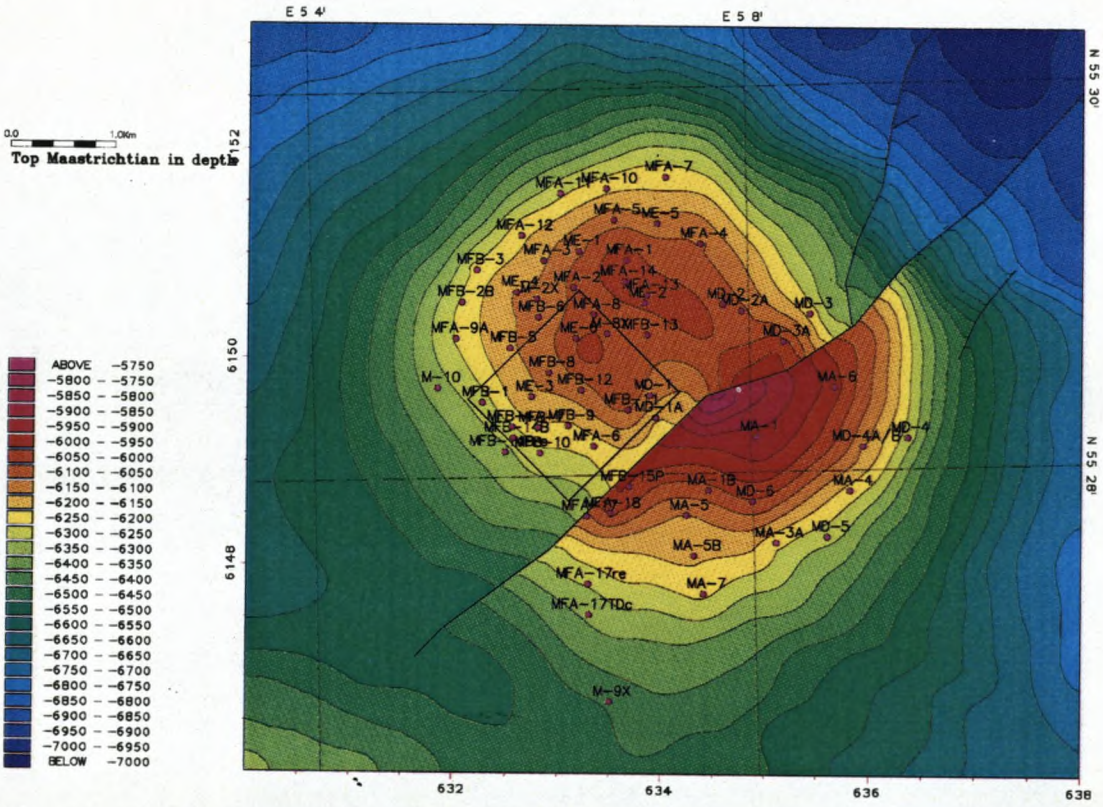

Figure 1: Top Maastrichtian with depths in feet (Kristensen et al 1995). The study area is shown by the box on the northwest side of the main fault.

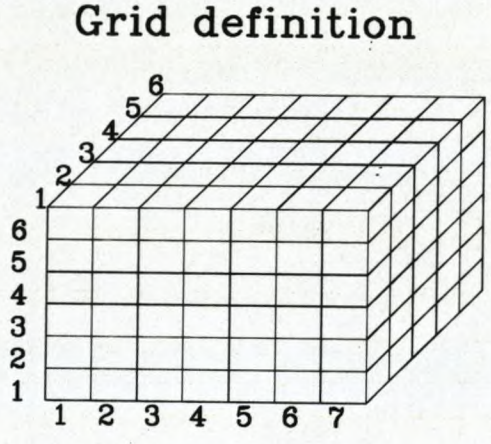

Figure 2: Definition of the reservoir characterization grid. The cell size is $25 \cdot 25 \cdot 6m$, and the grid contains $54 \cdot 61 \cdot 17$ cells.

There are two fundamental problems with obtaining good descriptions of the permeability distributions:

1. There are usually only very few permeability measurements because they are obtained through costly core analysis and require availability of core material. No logging tool can provide these data unambiguously.

2. Averaging is bound to produce errors, because extreme values in permeability control reservoir flow performance, either as barriers (low values) or by channeling flow (high values) depending on spatial continuity.

None of the 15 wells available within the volume have permeability measurements for the entire drilled section of the Maastrichian reservoir unit, and some do not have any permeability measurements at all. The problem of the few core analysis data is attempted to be solved by the application of a constructed bivariate conditioning dataset of porosity, permeability pairs in this report. The usually large population of porosity data from wells (in this case increased by the a priori porosity simulation) is thus utilized to constrain permeability description. The porosity/permeability data cannot be utilized directly through the construction of a least squared fitted curve, because this would not reproduce the spread in permeabilities. This is overcome by constructing a bivariate conditioning dataset, which is constraining simulation by defining the spread in permeabilities at all levels of porosity. This dataset encompasses all outliers that are accepted as representing matrix permabilities.

Results are illustrated by selected cross-sections and maps extracted from the resulting simulated permeability volume. In addition diskettes are provided with the porosity and permeability grid and the conditioning dataset (see appendix A). Even though a multitude of equiprobable realizations are possible, only one realization is made. Therefore no attempt has been made to investigate possible spread in solutions. Appendix B contains the parameter file with the design of the simulation.

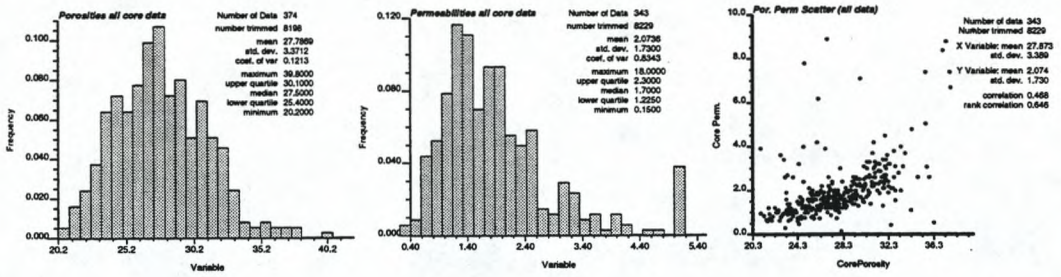

Figure 3: Total core porosity and permeability populations.

3 Data analysis

The main data here are core analysis derived permeabilities, and a priori simulated porosities. For details on the derivation of the porosities, the reader is referred to Vejbæk (1995). The simulation exercise in this report is aimed at providing permeability properties for cells of the size: $25 \cdot 25 \cdot 6m$. Core permeabilities are measured on plugs with sizes on the order of inches. Averaging is therefore needed. Averaging is, however, causing reduction in number of data, and an undesirable reduction in variance of data. There are only 374 samples from core analysis derived porosity measurements of which only 343 samples also have permeability measurements (Fig. 3). Some of the high permeabilities plot well away from the main body of data, and are disregarded as they are probably representing effects from fractures in the plugs. The goal of this modelling exercise is only to deal with matrix properties as fracture permeability is regarded as having a spatial structure more or less unrelated to the matrix structure.

Permeabilities cannot be averaged in a simple way like porosities, because extreme values tend to control flow, either as barriers for low values or by channeling flow for high values. Depending on whether these extremes are connected or not, they may therefore constitute important controls on flow. The organization of highs and lows with respect to flow direction is also of importance. If flow is parallel to bedding in a layered rock, an aritmetric average gives the best estimate, whereas if flow is perpendicular to bedding harmonic average gives the best estimate. Geometric average gives intermediate values corresponding to disorganized permeability distributions and/or flow at arbitrary angles to bedding. This is because the harmonic average tends to put emphasis on the low values, and the aritmetric average puts emphasis on the high values. The kind of average which most correctly describes average flow performance can best be determined from flow simulation studies.

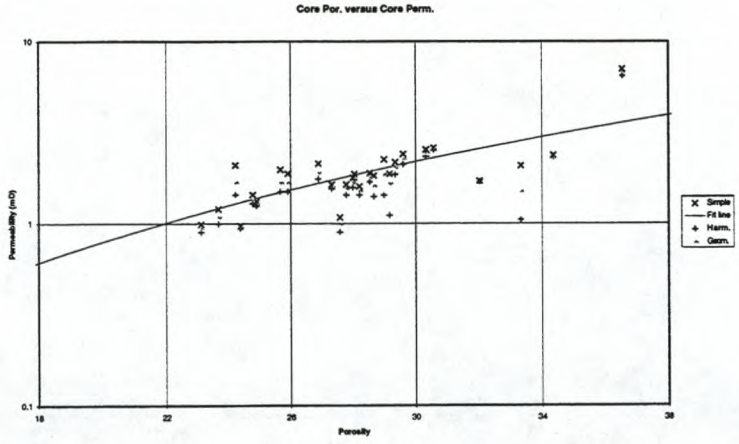

Figure 4: Block means of core porosity versus core permeability found by simple average, harmonic average and geometric average. The curve is a least squares fit to the data.

$$m_{si} = \frac{1}{n}\sum_n X \qquad \text{Aritmetrics average}$$

$$\frac{1}{m_{harm.}} = \frac{1}{n}\sum_n \frac{1}{X} \qquad \text{Harmonic average}$$

$$log(m_{geo.}) = \frac{1}{n}\sum_n logX \qquad \text{Geometric average}$$

The hard data boils down to 27 samples from the edited 343 samples, when averaged over the cells (Fig. 4). The spread in data within each cell mainly produces only minor discrepancies in the different types of averaging. The sets of different averaged values that relate to the same cell can be seen as three different symbols plotting at the same porosity value, but with different permeability value. The spread in these values relates to the heterogeneity within the cell, but also relates to the number of samples that went into the averaging of that cell.

A simple line fit of the aritmetric average of data to a function of the form $K = a \cdot \phi^b$, yields $a = 4.33 \cdot 10^{-4}$ and $b = 2.507825$ as shown on Fig. 4. Using only this line implies a very tight link between porosity and permeability, which even the few points available show is not present. There is still spread in permeability relative to porosity even though only one type of averaging is chosen. This spread is important to reproduce in the simulation. The different types of averaging only emphasize the ambiguous relationship between porosity and permeability.

The simulated population of permeabilities is three orders of magnitude greater (58072 samples), than the hard data population, which makes it highly unlikely that spread and variance of the target population (the whole volume) are represented in the sparse hard data population. The problem is emphasized by the demand for a correct permeability spread, even for small intervals of porosity. Given the small hard data population, the ambiguity in averaging technique and spread in data, it is deemed more likely that acceptable results will be achieved, if a subjectively constructed bivariate conditional distribution is constructed to guide the simulation.

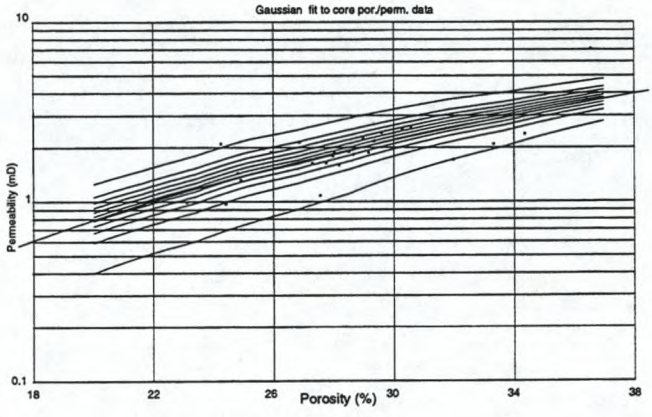

Figure 5: Block aritmetric means of core porosity vs. permeability data. The dashed curve is the least squares fit to the data, and the lines are manually fitted decile lines assuming gaussianity within each treshhold.

The construction of the bivariate conditional population has been controlled by drawing lines that define permeability decile distributions. These lines have been designed to be parallel to the least squares fit and to encompass all porosity/permeability outliers that were deemed valid representations of matrix properties. The deciles are designed to define a normal score distribution for a given porosity value (Fig. 5). The bivariate conditioning distribution is then constructed by drawing values with the a priori simulated porosities from within these classes and then assigning permeabilites according to a cumulative probability function for each porosity value as defined by the decile lines. It is not necessary to honour a normal score distribution for each porosity threshold, but there is too little data to indicate more sofisticated details for the relationship.

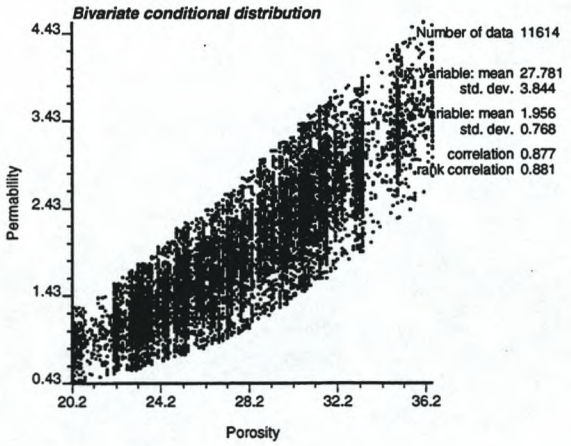

Figure 6: Resulting bivariate conditional distribution.

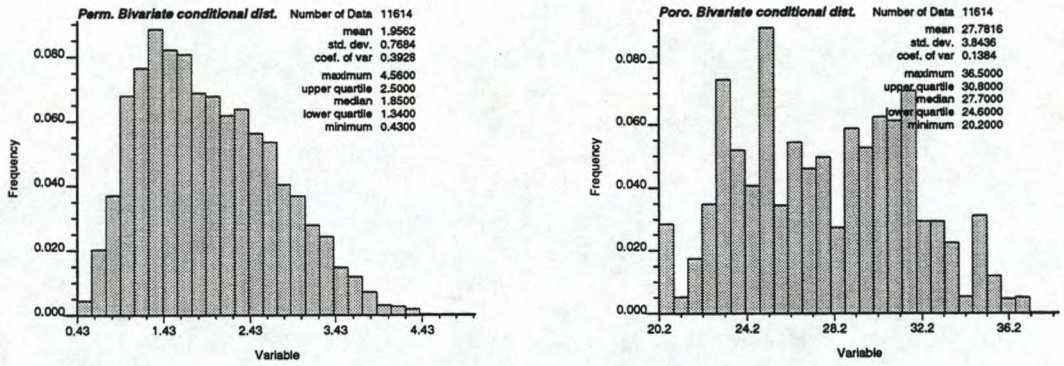

Figure 7: Histograms of the univariate distributions in the bivariate conditioning dataset.

The resulting bivariate population is seen in Fig. 6. The normal score distribution of permeability within porosity classes is visible as a more dense zone centrally in the cloud. This method also allows circumvention of problems with bias in the hard data population, because samples are produced for all cells that are being simulated. Comparison to the total data population (Fig. 3) also shows that no serious violation of the spread has been made, when outliers that are regarded as related to fractures are disregarded.

The resulting univariate distributions can be seen in Fig. 7. The variance is equal to the sill value of a variogram (in stationary populations). The variance of the hard data is probably not representative of the target population due to the very few samples. The variance from the histogram of the constructed conditioning permeability distribution (equals the squared standard deviation) is therefore regarded as a much better measure of what the sill value of the variograms should be than the variance of the 27 hard data points. The variance to guide the sill is therefore taken from the calculated bivariate conditional distribution. This has a standard deviation of 0.7684 corresponding to a variance of 0.549.

With only 27 hard data points, it is not possible to construct well defined variograms. Instead the variography obtained from the porosity simulation (Vejbæk 1995) is used with the sill value adjusted to equal the variance of the target population. This subjectively chosen variography may produce errors relating to the creation of too high or too low connectivity. With the relatively high correlation to porosity (0.877) it is considered that variogram ranges for permeability cannot be very different from those for the porosity. The ideal variograms are, however, unlikely to be exactly like the porosity variograms, because the correlation coefficient in not equal to 1.

The model variograms can be seen in Fig. 8 and sills and ranges are listed in Table 1.

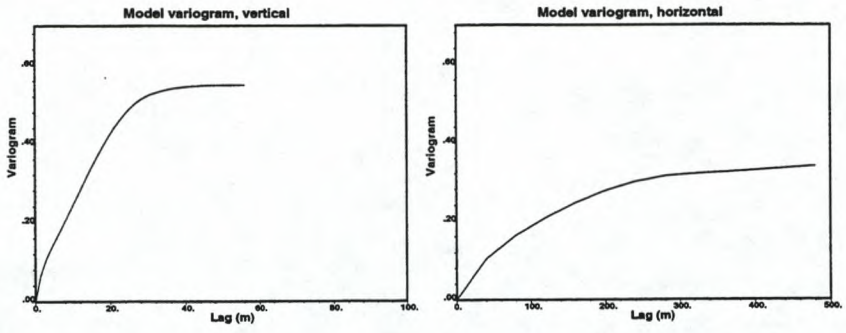

Figure 8: Model variograms used to constrain the spatial continuity of the simulated permeabilities.

Structure	Vertical ranges	Horizontal ranges	Sill value Hard data
Spherical	$30m$	$300m$	0.220
Exponential	$1.5m$	$30m$	0.082
Gaussian	$20m$	$650/1250m$	0.247

Table 1: Sills and ranges of the model variograms. Sill values add up to 0.549, which is equal to the variance of the constructed permeability distribution.

4 The ACS technique

The virtue of the ACS technique is to make use of a wider range of data and constraints than more conventional techniques allow (Deutsch and Journel 1992; Deutsch and Cockerham 1994). In the present study both hard data (core permeabilities) and soft data (a priori simulated porosities) are utilized via variograms and via constructed bivariate distributions.

The underlying annealing procedure is standard: initially the conditioning data is relocated to the nearest grid nodes and all remaining grid nodes are assigned values randomly chosen from the user specified histogram. This initial image is sequentially improved by swapping pairs of grid nodes that are not occupied by conditioning data. Swaps are accepted if the objective function is lowered, which is equivalent to improving the image. Swaps that increase the objective function are not all rejected, but accepted according to the so-called Boltzman distribution, which assigns a decreasing probability with decreasing 'temperature'; hence the similarity to freezing of a fluid.

The Boltzman distribution is given by the acceptance probability:

$$Prob\{accept\} = \begin{cases} 1 & \text{if } O_{new} \leq O_{old} \\ e^{\frac{O_{old}-O_{new}}{t}} & \text{otherwise} \end{cases}$$

As the temperature (t) is lowered, the probability for the second alternative decreases. This ensures that the optimization does not only find a local minimum and increases the chances for finding an optimal global solution to the objective function. The trick is then to find a sufficiently slow 'cooling' rate, and for each reduction in 'temperature' to have sufficient swaps to allow convergence. It has been found though, that for the purpose of cosimulation the sceme can be reduced to just rejecting all bad swaps and accepting all good swaps (Deutsch and Cockerham 1994).

The objective function is in the simplest case, a measure of the match between the variogram for the population ($\gamma^*(h)$) and a model variogram ($\gamma(h)$) given by the squared difference:

$$O = \sum_h \frac{[\gamma^*(h) - \gamma(h)]^2}{\gamma(h)^2}$$

where $\gamma^*(h)$ is the semivariogram for the population, $\gamma(h)$ is the prespecified variogram, and h are lag distances. The summation is taken over a prespecified number of lag distances. The denominator, which ensures a dimensionless value is not strickly necessary and is omitted in the sceme used here.

As stated previously, the annealing technique allows simultaneous honouring of a wide variety of data. This is done by extending the objective function to contain more components (c):

$$O = \sum_{n_c} w_c \cdot O_c$$

where O is the total objective function defined as a sum of all components, O_c is a component objective function, n_c is the number of components and w_c is a weight applied to that component.

In the present case there are also soft data in the form of presimulated porosity (Vejbæk 1995), and the bivariate distribution defining the link between porosity and simulated permeability (see below). These are honoured by discretizing the bivariate conditioning dataset into a set of cumulative distribution functions for permeability within each porosity class. The bivariate conditioning dataset in Fig. 6 is divided into porosity classes and for each porosity class a cumulative distribution function is build such that an equal number of permeability data points are found in each permeability class (Deutsch and Cockerham 1994). An element of the probability function can be written:

$$F(k_{i,j}, \phi_j) = Prob\,[K \leq k_{i,j}, \phi_j \leq \phi \leq \phi_{j+1}]$$

$$i = 1, ..n_k, j = 0, ...n_\phi$$

where n_k and n_ϕ are the number of permeability and porosity thresholds, K is permeability, and ϕ is porosity. Thus the objective function component which takes care of the soft data and the conditional bivariate distribution is:

$$O_{Biv.} = \sum_{n_k} \sum_{n_\phi} [F(k_{i,j}, \phi_j) - F^*(k_{i,j}, \phi_j)]^2$$

where F is the reference function, and F^* is the model (simulated) function. In the present case we use ten classes corresponding to nine thresholds for porosity classes, and for permeability classes within each porosity class (appendix B).

5 Results

The quality of the simulation result is depending on the ability of the simulator to reproduce the statistical characteristics specified in the design of the simulation (appendix B).

The histogram of the simulated permeabilities (upper left on Fig. 10) should be compared with the histogram of the conditioning univariate distribution (Fig. 7), which seems to be nicely reproduced both in terms of spread and shape. This is also the case with the conditional bivariate distributions, where the correlation coefficient is almost exactly reproduced (compare Fig. 10 middle left and Fig.6). The slight tendency for a step-like edge of the point cloud is because the bivariate conditional distribution is discretized into porosity intervals. It is interesting to see that the relative paucity of data (few data points) in both extremes of the plot of the simulated bivariate distribution is a reproduction of the conditional bivariate distributions (compare Fig. 10 middle left and Fig.6).

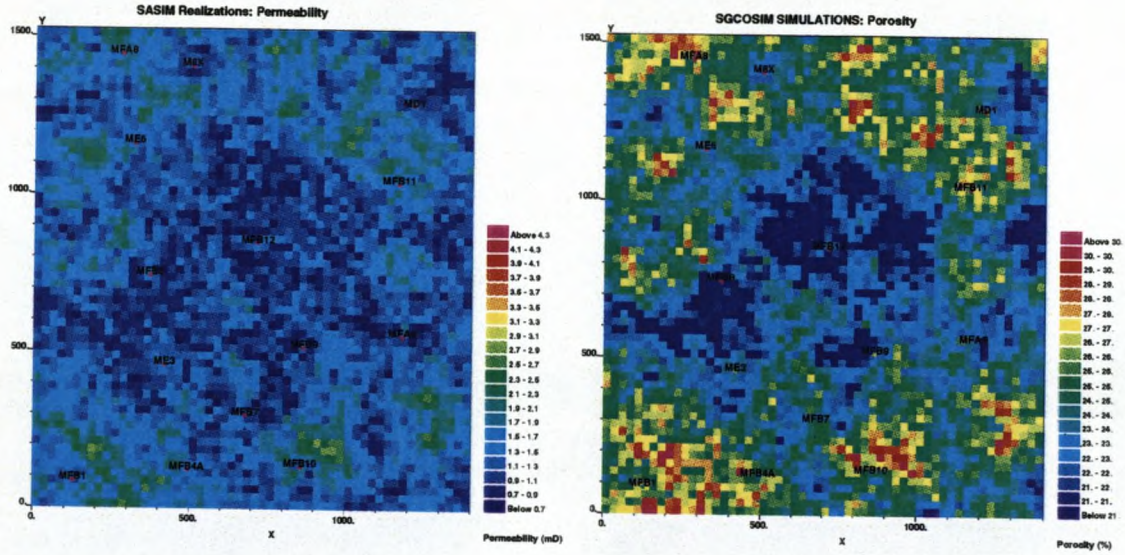

Figure 9: Map slices through the simulation volume at 3 m above base depicting permeabilities (left) and the a priori simulated porosities (right) that acted as soft data constraint in this report.

The reproduced correlation to porosity can also be seen by visual inspection of the maps and cross-sections shown in Figs 9, 11, 12, 13, and 14. The triangles shown on the cross sections are the conditioning hard data, where the colour inside the triangles corresponds to the hard data values. On the map sections the triangles merely shows the well location, not the conditioning data value. As porosities derived from logs were used to condition the porosity simulation, the triangles extend for the entire length of the well on the cross sections. The scarcity of core data is obvious from the permeability cross sections, where only few triangles are seen, and are even missing on Fig. 13.

The worst match in the realization relates to the variography as shown on the middle right, and the bottom plots on Fig. 10 (compare Fig. 8). Even though the selected model variograms are badly constrained by data and are subjectively chosen, they should theoretically be honoured by the simulation.

The sill values should be 0.549 as defined by the variance of the target population (see above) and specified in the simulation design (see appendix B). However, there is a strong vertical trend in the porosity data, which is visible in the porosity cross sections (Figs. 13 and 14) as discussed in Vejbæk (1995). The strong correlation between porosity and permeability (0.877; Fig. 6) causes the influence of the soft data to also produce a strong trend in the vertical output variogram. This is seen to be affected by the trend by having points plotting well above the sill value of 0.549 (Fig. 10 lower right). The long horizontal ranges specified in table 1, which also keeps the variogram below the sill within the displayed ranges are, however, honoured satisfactorily (compare Figs. 10 middle right and lower left and 8).

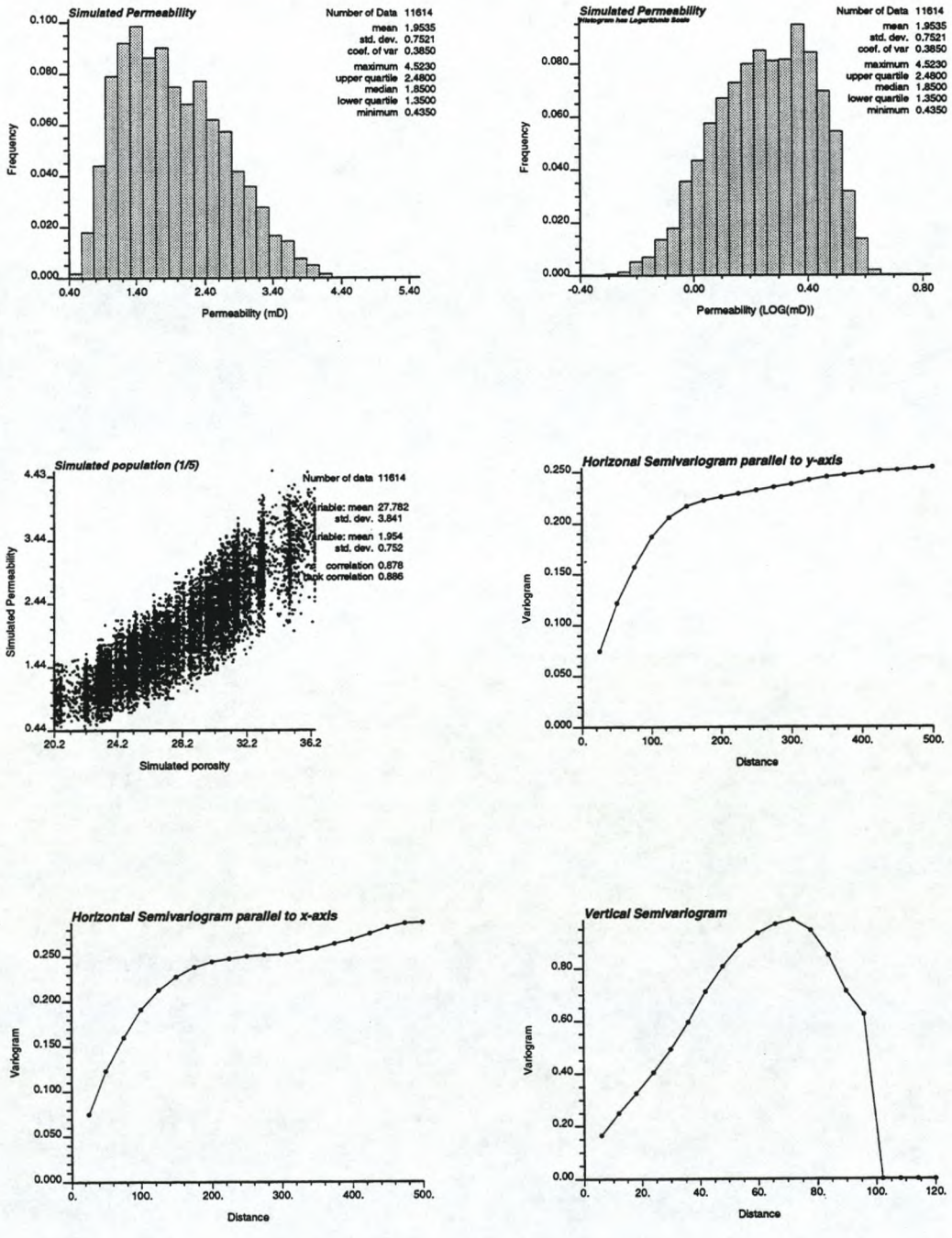

Figure 10: Summary statistics of the simulated permeability volume. See text for details

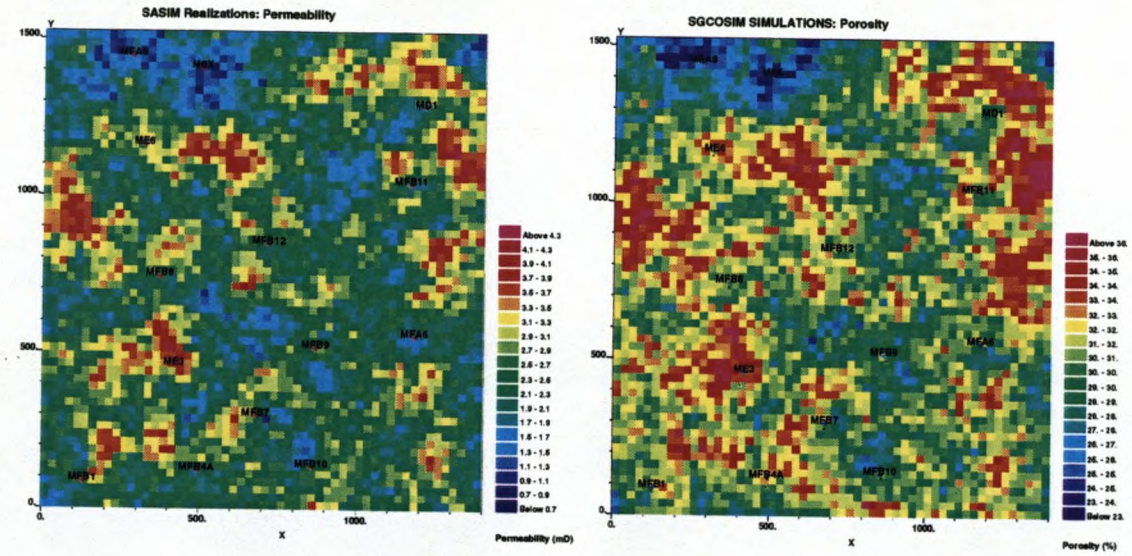

Figure 11: Map slices through the simulation volume at 63 m above base depicting permeabilities (left) and the a priori simulated porosities (right) that acted as soft data constraint in this report.

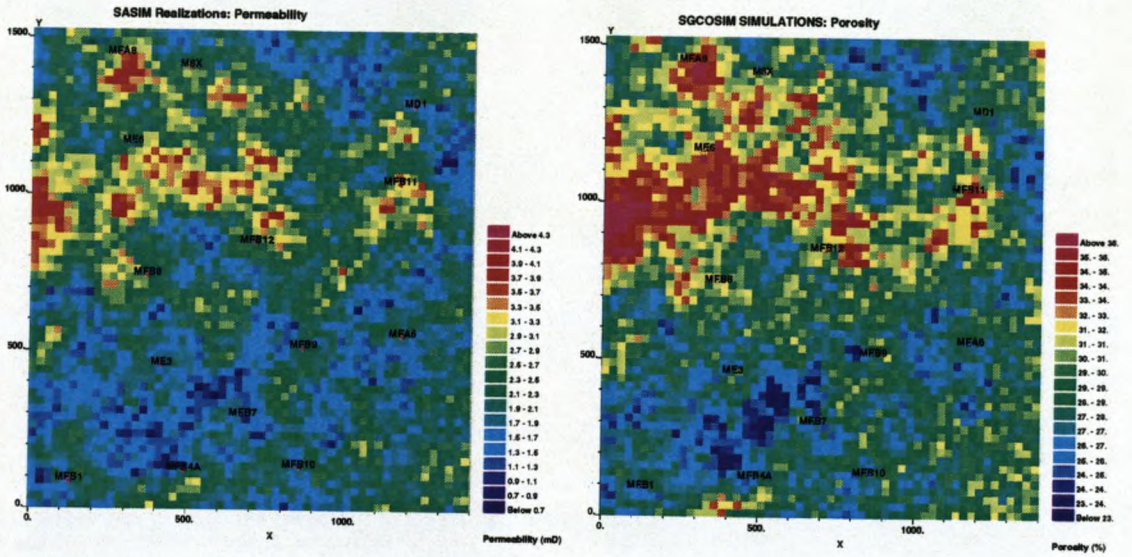

Figure 12: Map slices through the simulation volume at 99 m above base depicting permeabilities (left) and the a priori simulated porosities (right) that acted as soft data constraint in this report.

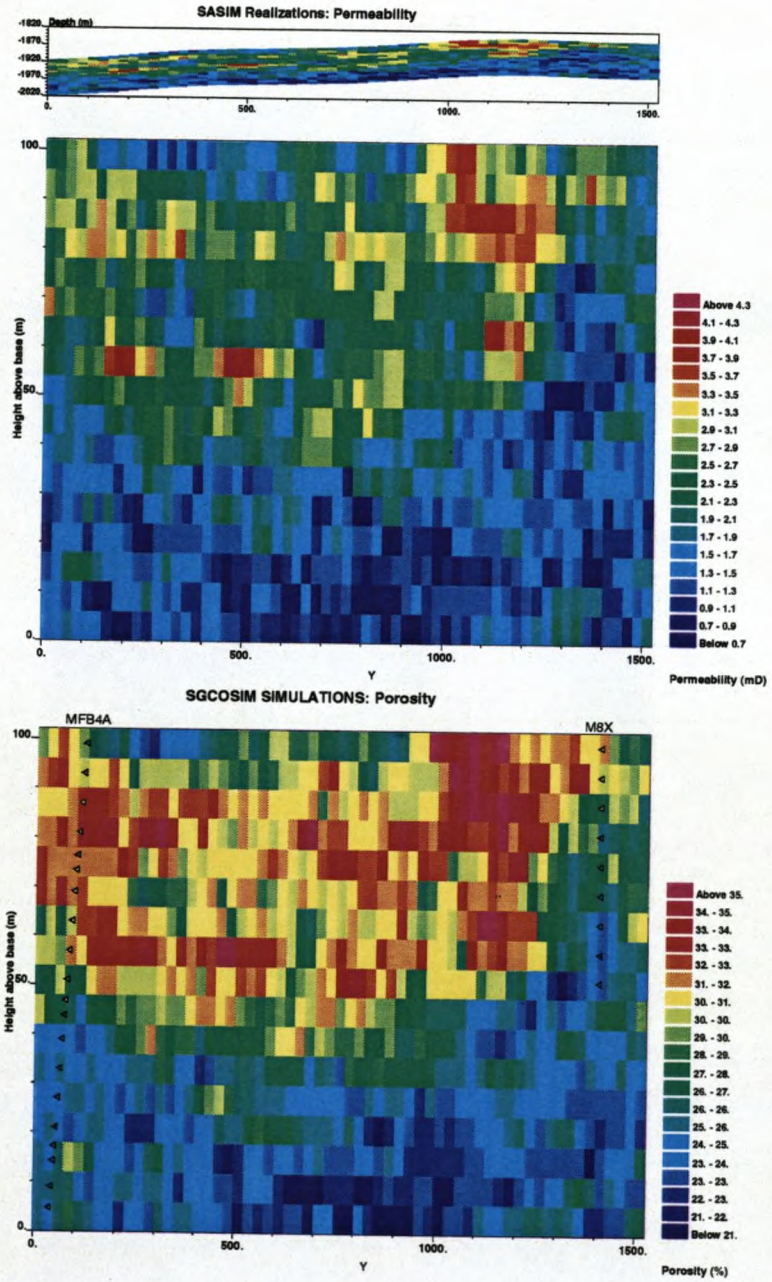

Figure 13: Cross section slices through the simulation volume at $x = 500$ depicting permeabilities (top two) and the a priori simulated porosities (below) that acted as soft data constraint in this report.

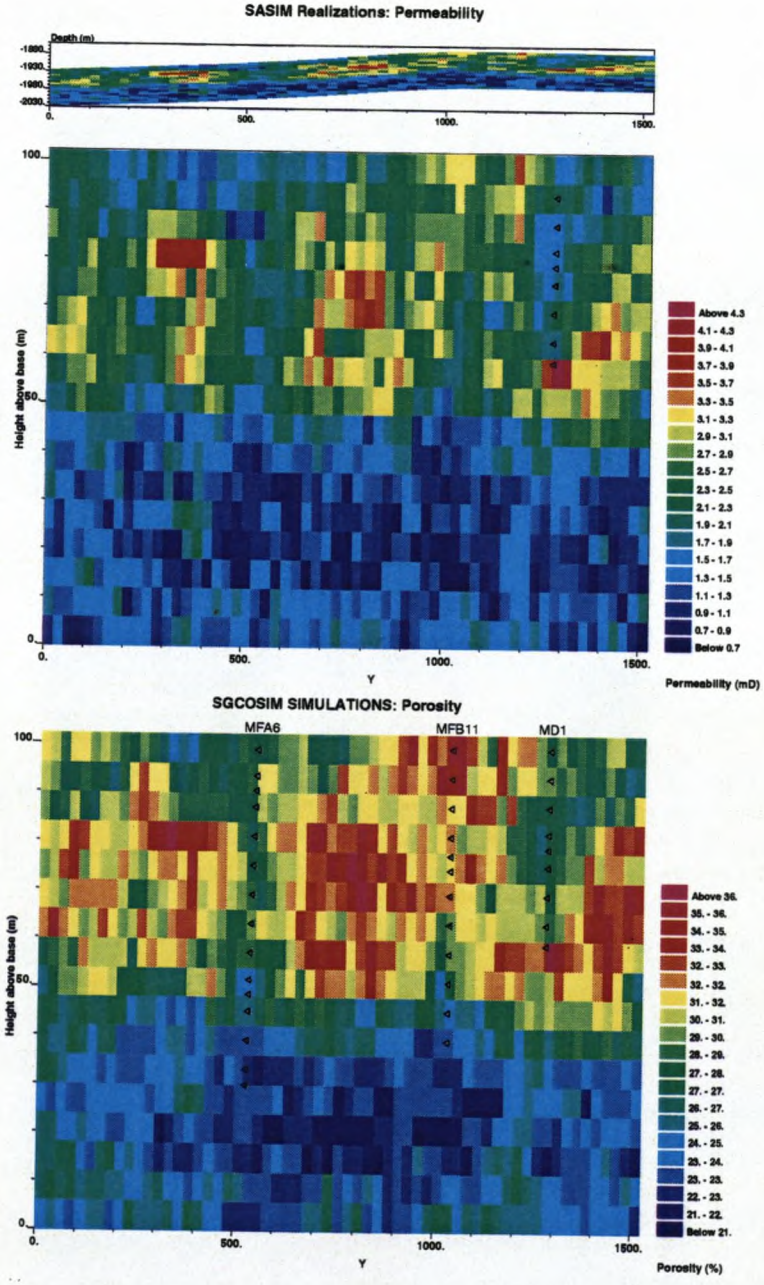

Figure 14: Cross section slices through the simulation volume at $x = 1200$ depicting permeabilities (top two) and the a priori simulated porosities (below) that acted as soft data constraint in this report.

6 Conclusion

The quality of a geostatistical model is directly related to how well it honours the available data. The ACS technique allows the simultaneous integration of many types of data. Even in ideal situations, where a multitude of high quality data are available, they are rarely adequate for unique determinations of reservoir properties. In the present case, however, data scarcity prevails. If we were to rely only on the available data, we would get results that would not satisfy our prejudice on how porosity and permeability covariate in space. The ACS method allows any such prejudice to be honoured through the possibility for specifying an expected bivariate behaviour. We thereby get permeability estimates also in wells, where only porosity data are available, and in a way that is consistent with these data, the neighbouring wells, and even with seismic impedances, which were used as support for deriving the porosity field.

7 References

Deutsch, C. V. and Cockerham, P. W. 1994: Geostatistical modeling of permeability with annealing cosimulation (ACS). SPE 28413, 523-532.

Deutsch, C. V. and Journel, A. G. 1992: GSLIB, Geostatistical software library and user's guide. Oxford University press, New York, 340 p.

Jørgensen, L. N. 1992: Dan field - Danish North Sea. In E. A. Beaumont and N. H. Foster (eds.): Structural traps VI, Atlas of oil and gas fields: Am. Ass. Petr. Geol. Treatise of Petroleum Geology: 199-215.

Kristensen, L., Dons, T., Maver, K. G. and Schiøler, P. 1995: A multi-disciplinary approach to reservoir subdivision of the Maastrichtian chalk in the Dan Field (Danish North Sea). Am. Ass. Petr. Geol. Bull. 79(11), 10 p.

Vejbæk, O. V. 1995: Stochastic modelling of porosity using seismic impedances on a volume of chalk in the Dan Field. Report to project EFP-95 1313/95-0005. DGU service report no. 61. 45 p.

Vejbæk, O. V. and Rasmussen, K. B. 1996: Geostatistical reservoir characterization using inverted seismic data: application to a chalk reservoir, Dan Field, Denmark. SPE 35486, 10 p.

8 APPENDIX A

The attached diskette is a DOS formattet 1.44 MB diskette containing one realization of the porosity permeability distribution in the volume shown in Fig. 1. The file is compressed from app. 4.7 MByte using the ARJ software to app. 0.9 MByte. The file format of the inflated file is the GSLIB format as described in Deutsch and Journel (1992). The format is basically free format ASCII files (first 20 lines):

```
SASIM Realizations
          9
X-UTM
Y-UTM
Depth
Neg. Depth
X
Y
Z_to_bot
Sim. Perm.
Sim. poro.
  632132.19 6149605.00  2016.7 -2016.7    12.5    12.5     3.0   1.5300  25.333
  632149.88 6149587.00  2016.6 -2016.6    37.5    12.5     3.0   1.4850  26.526
  632167.63 6149569.00  2016.4 -2016.4    62.5    12.5     3.0   1.5100  27.052
  632185.31 6149552.00  2016.1 -2016.1    87.5    12.5     3.0   1.4200  27.314
  632202.88 6149534.00  2016.1 -2016.1   112.5    12.5     3.0   1.6300  27.755
  632220.63 6149516.00  2016.0 -2016.0   137.5    12.5     3.0   2.1900  29.728
  632238.31 6149499.00  2015.8 -2015.8   162.5    12.5     3.0   1.9000  29.688
  632255.88 6149481.00  2015.4 -2015.4   187.5    12.5     3.0   2.0300  27.394
  632273.63 6149463.00  2015.1 -2015.1   212.5    12.5     3.0   1.0900  28.746
   .
   .
   .
```

The two first parameters (`X-UTM` and `Y-UTM`) are UTM coordinates referring to UTM zone 31 (meridian 3°) using Heyford 1909 spheroid. The depth coordinates (`Depth` and `Neg. Depth`) are true vertical depths in meters below mean sealevel. The coordinate parameters (`X`, `Y` and `Z_to_bot`) are coordinates that refer to the carthesian grid system in which simulation took place. They refer to distance from the lower western corner of the volume: `Z_to_bot` is height above the base of the volume, `X` is increasing in a southeastern direction, and `Y` is increasing towards the northeast. The data are ordered according to this coordinate system counting first along the x-axis, then row by row along the y-axis, then layer by layer along the z-axis. The parameters `Sim. Perm.` and `Sim. poro.` are the simulated permeabilities in milli Darcy as described in this report and the best case porosities in pct. according to Vejbæk (1995).

The number of grid cells are 57 in the X direction, 61 in the Y direction, and 17 in the z direction. The cell size is $25 \cdot 25 \cdot 6m$ with the points referring to the center of the cells. The lower left point in fig. 2 is thus at location: $x = 12.5m, y = 12.5m, z = 3m$. Grid dimensions are accordingly: $1400m \cdot 1525m \cdot 102m$.

The conditioning data file is called `hardper3.dat` and is also of the GSLIB formatted type. The header below is explained in the right column:

`Blokaverage of ../tomaa1-6.dat`	Header
`15`	Number of variables
`X-coor`	X-coordinate in model
`Y-coor`	Y-coordinate in model
`Trace`	Seismic trace nr.
`Line`	Seismic Line nr.
`ZtoBot`	Height above base of volume
`-ZtoBot`	Height above base of volume
`TVD`	Depth below mean sea level
`-TVD`	Depth below mean sea level
`CorePorosity`	Core porosity
`Saturation`	Water saturation
`Porosity Log`	Porosity from log data
`Core Perm.`	Aritmetric average permeability
`Harm. Perm.`	Harmonic average permeability
`Geom. Perm.`	Geometric average permeability
`Simulated Porosity`	Simulated porosity

//[4mm] The value defining missing values is -999. The total dataset in the file `tomaa1-6.dat` is similarly organized in the GSLIB format:

`Transf= flat ZtoTOP-Maastr.`	Header
`13`	Number of variables
`X-coor`	X-coordinate in model
`Y-coor`	Y-coordinate in model
`Trace`	Seismic trace nr.
`Line`	Seismic Line nr.
`ZtoTop - m`	Height above base of volume
`ZtoTop - ft`	Height above base of volume
`ZtoMaa - m`	Height above base of volume
`Z TVD - ft`	Depth below mean sea level
`CorePorosity`	Core porosity
`Core Perm.`	Core permeabilty
`Log Porosity`	Porosity from log data
`Saturation`	Water saturation
`impedance`	Seismic inversion impedance

9 APPENDIX B

The parameter file used for SASIM is shown below.

```
                  Simulated Annealing Based Simulation
                  ************************************

START OF PARAMETERS:
0  1  0  1  1                          \components: hist,varg,ivar,corr,bivh
0  3  0  1  1                          \weight:     hist,varg,ivar,corr,bivh
0                                       \0=no transform, 1=log transform
1                                       \number of realizations
56     12.5   25.0                      \grid definition: nx,xmn,xsiz
61     12.5   25.0                      \                 ny,ymn,ysiz
17      3.0    6.0                      \                 nz,zmn,zsiz
260357                                  \random number seed
4                                       \debugging level
dbg.sasim                               \file for debugging output
sasim.out                               \file for simulation output
1                                       \schedule (0=automatic,1=set below)
1.0   0.1   75  8  3 0.00001           \   schedule: t0,redfac,ka,k,num,0
200.0                                   \   maximum number of perturbations  10.0
0.1                                     \   reporting interval
1                                       \conditioning data:(0=no, 1=yes)
hardper3.dat                            \   file with data
1   2   5  12                          \   columns: x,y,z,attribute
-90        1.0e21                       \   trimming limits
0                                       \file with histogram:(0=no, 1=yes)
../data/cluster.dat                     \   file with histogram
3   5                                   \   column for value and weight
99                                      \   number of quantiles for obj. func.
1                                       \number of indicator variograms
2.78                                    \   indicator thresholds
../bestsim/sgcosim.out                  \file with gridded secondary data
1                                       \   column number
0                                       \   vertical average (0=no, 1=yes)
0.877                                   \correlation coefficient
cdpope.out                              \file with bivariate data
2    1    0                            \   columns for primary, secondary, wt
0.01    5.0                             \   minimum and maximum
9                                       \   number of primary thresholds
9                                       \   number of secondary thresholds
60                                      \Variograms: number of lags
0                                       \   standardize sill (0=no,1=yes)
3    0.00                               \   nst, nugget effect
2    0.0824  0.0   0.0   0.0           \   it,cc,ang1,ang2,ang3
           30.0  30.0     2.0          \   a_hmax, a_hmin, a_vert
1    0.21976 0.0   0.0   0.0           \   it,cc,ang1,ang2,ang3
          300.0 300.0    30.0          \   a_hmax, a_hmin, a_vert
3    0.24723 90.0   0.0   0.0         \   it,cc,ang1,ang2,ang3
         1250.0 650.0     20.0         \   a_hmax, a_hmin, a_vert
```